A Feasibility Study of a Load Sensor to Measure Weight Bearing in Pediatric Standers

By

Joshua Runako Daniel

Sc.B., Brown University, 2018

Thesis

Submitted in partial fulfillment of the requirements for the
Degree of Master of Science in Biomedical Engineering at Brown University

PROVIDENCE, RHODE ISLAND

MAY 2020

This thesis by Joshua Runako Daniel is accepted in its present form
by the Center of Biomedical Engineering as satisfying the
thesis requirement for the degree of Master of Science.

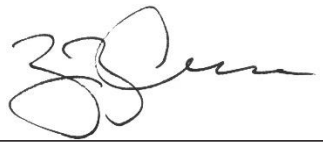

Date 04.30.20

Dr. Joseph Crisco, Advisor

Recommended to the Graduate Council

Date 04.30.20

Dr. Christopher Bull, Reader

Date 04.30.20

Dr. Jonathan Schiller, Reader

Approved by the Graduate Council

Date 04.30.20

Dr. Marissa Gray, Biomedical Engineering Master's
Program Director

Acknowledgements

I would like to thank Dr. Joseph Crisco for his guidance, and encouragement throughout the evolution of this project over the past two semesters. I appreciate the facilitation and direction of my pursuit of entrepreneurship activities to complement my coursework and thesis development.

I would also like to thank Cynthia Chrostek, Dr Jonathan Schiller and Prof Chris Bull for their assistance in having this thesis meet significant clinical and technical milestones so rapidly.

The team at Bay Computer Associates has done an excellent job in developing electronic components and communicating progress and functionality in a timely way. Thank you, Ben Lyons, for your help in machining these sensors.

This project builds on the work completed over the past few years by Mikayla Tinus, Madison Kuhn, Dana Leichter and Matthew Navarro. Your insight and well documented activities were significant to the progress of this work. I am grateful to all the physical therapists and administration at Meeting Street and Hasbro Children's Hospital that have been instrumental in this device's development.

Finally, this work would not have been possible without the support and encouragement of my parents, brothers and friends. Thank you so much for your unending love. I am truly blessed to receive it.

Table of Contents

Introduction

Background and Motivation

Persons afflicted with neuromuscular conditions, whether acute, due to stroke, spinal cord injury or other traumatic events, or congenital such as cerebral palsy (CP) and duchenne muscular dystrophy, frequently suffer from secondary musculoskeletal conditions. These conditions may be so severe that they prevent persons from walking or standing unassisted. The consequences of this include significant body structure and function impairments such as altered muscle tone or spasticity, range of motion (ROM) limitations or contractures, muscle weakness, constipation, decreased bone mineral density (BMD) with increased risk for fractures and bone pain, as well as activity limitations and participation restrictions. These conditions can result from long-term sitting and lying postures in those with chronic conditions. However, these conditions also impact individuals in the sub-acute phase a few weeks after onset of disease or injury (1–4).

Cerebral palsy is one of the common neuromuscular diseases that is treated with assisted standing therapy and is the most common motor disability in childhood (5). Population-based studies from around the world report prevalence estimates of CP ranging from 1.5 to more than 4 per 1,000 live births or children of a defined age range (5). CP is a chronic central nervous system disorder for which no cure exists, and so current treatments, whether surgery, therapy, or medications, aim to alleviate such peripheral effects on the musculoskeletal system as muscle tightness, decreased BMD and spasticity (6). Assisted standing therapy has also been used to treat adult populations who have suffered from strokes, as they are also subject to large bouts of inactivity (4). Every year, more than 795,000 people in the United States have a stroke (7), and approximately 35 percent of survivors with initial paralysis of the leg do not regain useful function, and 20 to 25 percent of all survivors are unable to walk without full physical assistance (8).

Assisted standing for non-ambulatory individuals, using a standing device or stander, has numerous, well-documented benefits that include both psychological and physiological factors. Assistive standing devices, such as standers, tilt tables and sit-to-stand wheelchairs support the user in positioning and prolonging a standing or partial standing position. These devices also commonly stabilize hips, knees and ankles using strappings at the chest, heels, knees and hips (4). These devices are generally classified into dynamic and passive; the former allowing motion while the latter are stationary, with each category having a range of designs. These designs include prone and supine support, and other features such as footplates that can be adjusted laterally to enable different angles of hip abduction. Figure 1 highlights the range of stander designs, and modifications.

Figure 1: Stander Designs (9)

Many studies have highlighted the benefits of standing, and Figure 2 illustrates this range. These include benefits to bowel and bladder function with a significant ($p < 0.05$) increase in frequency of bowel movements and a decrease in bowel care time with the use of the standing table 5 times/week versus baseline (10), skin integrity, in a 2001 study that highlighted that subjects with spinal cord injuries reported perceived effects benefits to skin integrity and limiting bed sores (11), cardio-respiratory health, through increased hypertensive tendencies noted by the 3rd day of non-participation [in therapy program] (12), and psychological health and general wellbeing (11).

Duration and magnitude of mechanical loading plays an important role in skeletal health, and this is a major reason standing devices are widely used with non-ambulatory persons. The implications to bone mineral density was shown by a study concluding that a longer period of standing in non-ambulant

children with CP improves vertebral but not proximal tibial volumetric Trabecular(VT) BMD (13) and that passive mechanical loading can have a beneficial effect on the preservation of bone mass in osteoporosis (14). Additionally, evidence suggested that long-term, higher dose programs may slow bone loss (15).

Spasticity and gait are also supported by assisted standing therapy. A 2010 study demonstrated that the gait pattern of children with cerebral palsy classified as level II or III on the Gross Motor Functional Classification System (GMFCS) – a 5 level categorization tool for the gross motor function of children and young people with cerebral palsy- improved through the implementation of a prolonged standing program (16). Additionally, standing has been shown to be more effective than no treatment and as effective as night-time splinting in preventing ankle contractures in subjects with stroke (17). Muscle strength and function has also been shown to improve through assisted standing (18). A 2007 study indicated that subjects actively responded to exercise dynamic weight bearing, as measured by electromyography (19).

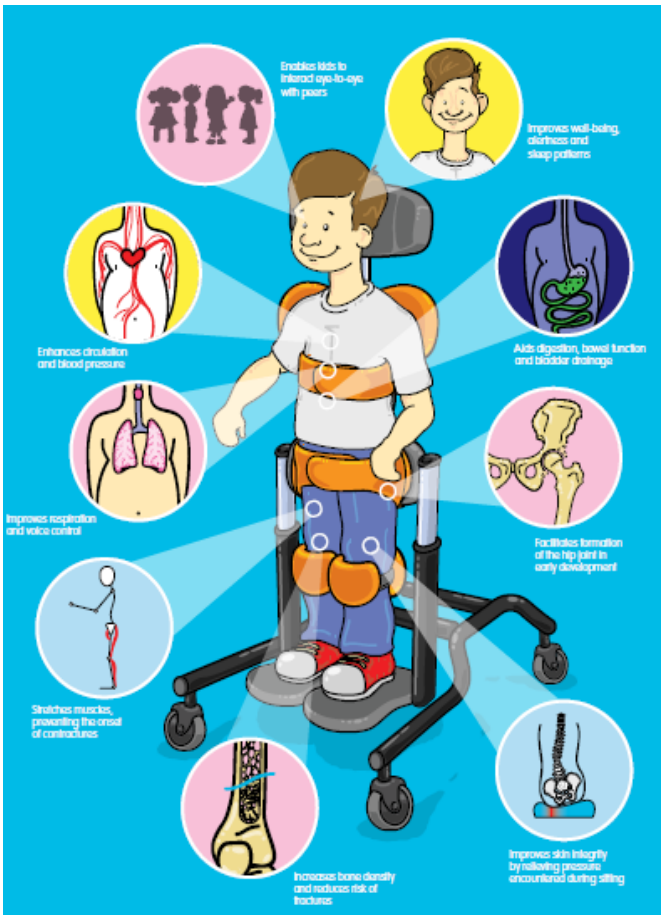

Figure 2: Benefits of standing (graphics provided by ottobock in partnership with Leckey)

Duration and magnitude of mechanical loading plays an important role in skeletal health, and this is a major reason standing devices are widely used with non-ambulatory persons. However, little is known about the true axial loading that occurs while in a stander, or the factors which may impact loading. A 2007 study highlighted that weight-bearing ranged widely (23%–102%) with a mean of 68% of body weight, along with was some variation over the course of a session and between different sessions, but more variance noted between subjects. It concluded that actual weight borne in a stander is quite variable, and in some instances only a fraction of actual body weight (20). Similarly, a 2008 study that investigated continuous load bearing over multiple standing sessions in 20 participants with (GMFCS) Level IV and V, found that weight bearing ranged widely from 37 to 101% of body weight. Furthermore, examination of the difference between weight bearing between right and left sides found that the absolute difference was as much as 40% in their sample of therapy sessions (21).

These studies, along with others recommend that further research be conducted to determine specific “dosing” for standing programs to create long-lasting functional effects (16,20,21). Interviews and observations with physical therapists (PTs) operating at Meeting Street in Providence, Hasbro Children’s Hospital, Rhode Island public school districts and a leading researcher in pediatric weight bearing has continued to highlight this. As part of the New England Regional National Science Foundation Innovation Corps (NSF I-Corps) Spark Program towards innovation discovery has further confirmed the reliance on the attending PT’s judgment to estimate the level of weight bearing, using visual investigation or placing their hands beneath the patient’s feet. Of course, these methods are not accurate, precise nor repeatable. These methods also do not allow for tracking of weight bearing in real time, measurement of the level of weight bearing, nor how the points of weight-bearing may change throughout the course of a standing session and over several sessions. A tool that can serve these purposes, has therefore been identified as being potentially highly valuable to the quality of care delivered to non-ambulatory persons, in that it would facilitate the delineation of the relevant factors of weightbearing, which in turn may suggest ways to maximize weightbearing loads while in a stander (20).

Comparable technology

Currently marketed products that are comparable in nature include the Rifton TRAM and the BiSym Scale from LiteGait. The TRAM is a transfer and mobility device outfitted with a scale that can connect with a phone or tablet via Bluetooth to display scale data on its Gait Tracker app. The app tracks a 10-second average of the weight measured by the scale and provides the average weight-bearing of a gait training session. At present the scale option must be chosen at the time of the original purchase, cannot be added later and is compatible only with the TRAM. The Rifton TRAM costs $4900.00, is sizeable at 43 inches tall and weighs 70 pounds (22). The BiSym Scale measures unilateral or bilateral support. The harness system is outfitted with a yoke which holds the patient’s arms above each shoulder. This system can be adjusted to provide variable support on each side from full to no support, and sensors measure and report the weight bearing load changes from the right to left side during the gait cycle (23).

Though these devices emphasize the potential market value and clinical use of a weightbearing tracker, they are not practical for use during stander therapy as they are extremely sizeable gait trainers with a hefty price tag that could significant distract from other surrounding activities such as classroom learning. The lengthy set up time along with reduced mobility and adaptability limit adoption to assisted standing therapy, but highlights the necessity for wireless data transmission and readings for each foot's loading.

Design Requirements

The following design requirements were primarily identified based on interviews with Meeting Street physical therapists. Fifteen additional interviews completed as part of the New England Regional National Science Foundation's Innovation Corps (NSF I-Corps) further defined these requirements. These were completed with Rhode Island physical therapists based at Hasbro Children's Rehabilitation Center, Warwick School District, Easterseals Early Intervention program in January and February 2020.

At present, these 26 requirements are at different levels of validation with the current prototype. Additionally, there are requirements that have not yet been defined, but they address device features necessary for successful and safe adoption and use. Rationale for each requirement is also listed below.

Requirements satisfied or testable with current prototype.

1. Report loads up to 686N (70kg+/-1.4 kg)
    - Based on weight of pediatric patients requiring assisted standing therapy
2. Report loads with a mean accuracy of 2% over 5 trials within the range of 0.0 to 686N (70kg)
    - Approximate accuracy desired of device, to be further validated.
3. Report 60 mins (+/-1.2) of continuous loading from 0kg to 588N (60kg) at a rate increase of 9.88 N/min (1kg/min)
    - Based on duration of therapy session
4. Set up time less than 5 minutes +/- 0.5 mins after 2 tutorials

- Based on workflow requirements

5. Removal time less than 5 minutes +/- 0.5 mins after 2 tutorials
    - Based on workflow requirements
6. Energy requirements: standard voltage is 120 V and the standard frequency is 60 Hz or through connection to Micro USB. to computer
    - Based on regularly accessible power connection in rehabilitation facilities.
7. Tolerate maximum loading of 785N (80kg +/- 2 kg)
    - Based on potential maximum loading
8. Through visual inspection, surfaces must be flat without sharp edges.
    - Based on device's exposure to children and potentially exposed skin.
9. Battery pack must be IEC 62133 approved.
    - Standard that specifies requirements and tests for the safe operation of portable sealed secondary cells and batteries used in medical equipment.
10. The surface of the sensor must be chemically passive.
    - Based on device's exposure to children and potentially exposed skin.
11. Weigh less than 20N (2kg +/-0.2kg)
    - Based on frequency of use and portable nature
12. Height less than 0.0254m
    - Based on frequency of use, portability and low profile desired.
13. Surfaces must be sanitized with bleach or disinfectant with 70% alcohol
    - Based on reusable requirement and environmental exposure

Requirements not yet achieved by prototype

14. Bluetooth range of data recording must be 3 meters +/-0.3m

- Based on frequent use case of in-class therapy, thereby limiting distraction caused by PT monitoring therapy

15. Wireless transmittance of data to iOS app
    - Based on desire by PTs for real time monitoring of patient weight bearing to mobile phone
16. Ability to save data for future review.
    - Based on desire by PTs for long term tracking of patient weight bearing

Other requirements

Listed here are other requirements that have not been fully defined at present but are anticipated to be necessary towards device adoption.

17. Battery life of 8 hours +/- 0.5hours
    - Based on frequency of use within a day of use.
18. Charging time of 2 hours
    - Based on common daily workflow in facilities of use.
19. Electrical components insulated and not subject to environmental damage
    - Based on desire for infrequent replacement of device, and safety requirements
20. Maintain functionality following 3 drop tests of 2 meters.
    - Based on storage sites within facility of use and portable requirements
21. Maintain functionality within humidity range of 40% and 60%
    - Based on approximate humidity anticipated in facilities of use
22. Maintain functionality temperature range of 15 and 30 degrees Celsius
    - Based on approximate temperature anticipated in facilities of use
23. Under designated use, must have a lifespan of 2 years +/- 0.2 years, or 4000hours +/- 400 hours of use, whichever elapses first.
    - Based on desire for infrequent replacement of device
24. Battery cycles to be determined

- This requirement implicates the lifespan of the device

25. Cost to be determined

- This requirement implicates the accessibility and feasibility of adoption

26. Training time to be determined

- This requirement affects the time for adoption and implementation across rehabilitation facilities

Project Overview

This project is the initial design, development, testing and feasibility study of a sensor to measure the extent of load bearing by patients undergoing assisted standing therapy. The Sensor used in this study is intended to be used as a tool to measure and record the magnitude and time period of load bearing for persons undergoing routine stander therapy.

This technology gives the attending physical therapist, researchers and clinicians a means of monitoring the extent of load bearing within a stander therapy session and over multiple stander therapy sessions. Load bearing helps generally in bone density development and stimulating muscle growth; however, this tool is intended to assist in measurement of load bearing, though physical therapists present could utilize the real time weightbearing data to make adjustments to the patient's positioning and the stander configuration.

This sensor at its core leverages 4 load cells connected to a printed circuit board, all sandwiched between 2 aluminum plates. The load cells are offset from the surfaces of the aluminum surfaces and deform accordingly to an applied load. This deformation is translated to an electrical signal that can be calibrated, and thereby used to identify magnitude of the weight applied. The sensor is currently internally outfitted with an is IEC 62133 approved internal battery and enclosed by an external gasket made from a proprietary thermoplastic polyurethane (TPU) chosen for its durability and flexibility. Further iterations of this sensor incorporate features necessary to commercial viability. This include a wireless transmittance of data and ability to save data future review.

From the Bland Altman analysis of the agreement between the calibrated sensor weights and the applied deadweights, there is relatively strong agreement among smaller weights, with larger variation among heavier weights. As these initial tests were conducted using dumbbell deadweights, repeating this process and exploring the agreement using a calibrated system, such as the Instron Universal Testing System will is necessary.

To validate the feasibility of this design and this sensor's use, a 15-person feasibility study utilizing these sensors has secured Institutional Review Board approval from the Rhode Island Hospital. It was reviewed as a low risk pediatric study and the load sensor plate was granted an NSR (non-significant risk) determination based on the Instructions for Use documentation developed. Additionally, study enrolling a control group of fully ambulatory children aged 8-17 years old of matched weight and height has also been approved to test the accuracy of the sensor's by standing on the sensor in various loading positions.

Following this feasibility study, long term clinical study must be designed and executed. The structure of this study will need to highlight, through use of the sensor, the dosing (time and magnitude) of weightbearing that facilitates improvement in physiological outcomes vital to the quality of life of the patient. At this moment, bone mineral density, muscle strength, hip mobility and spasticity are the outcomes that will be explored in a long-term study. A matched cohort study would potentially highlight the advantage of using this device to the outcomes described above.

Commercial viability of the project is currently being explored through participation in a series of University sponsored accelerators, Med -Tech commercialization programs and customer discovery programs (NSF I-Corps). These programs will set the foundation for a pursuit of venture capital and federal research grants to support the continued advancement of this project.

Sensor Design

Weight sensors that are placed between the foot of the patient prescribed assisted standing therapy and the base platform of the standing device have been developed (Figure 3). At this stage, user communication with the device is over a simple ASCII interface using the USB serial connection. A free serial terminal program called PuTTY, which runs on MacOS/Windows/Linux is utilized and the hardware interface between the device and computer requires a USB A Male to Micro B cable. This design has been an advancement of the work of Madison Kuhn, Mikayla Tinus and Dana Leichter during the ENGN 1930L senior capstone design course in Fall 2017. Additionally, Bay Computer Associates has managed the development of all electronic components.

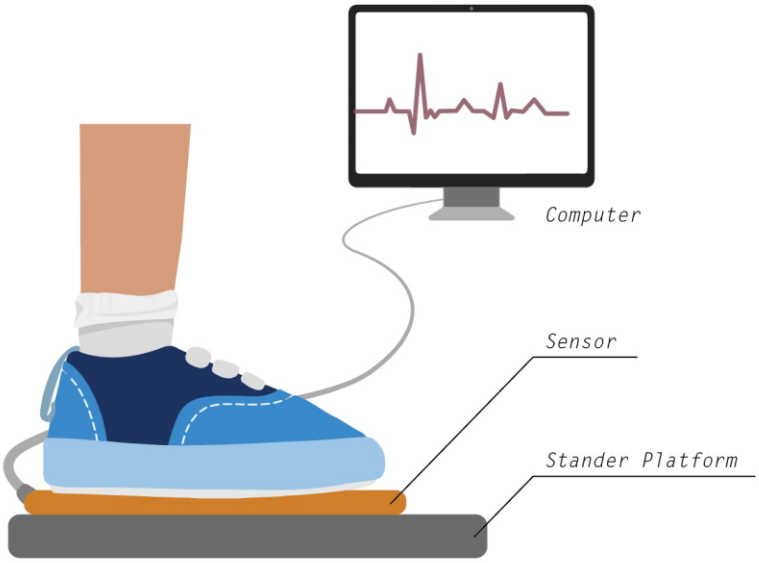

Figure 3: Current prototype of sensor, with wireless transmission to a mobile app in future iterations.

The sensor's geometric form was informed by measuring dimensions of 12 pediatric standers available at Meeting Street in July-August 2019 by Alpert Medical School student Matthew Navarro MD'22, under the supervision of physical therapists. Specifically, the sensor's dimensions had to fit within the perimeter of the standing platform for each stander (Appendix 1). Additionally, the absence of a single base plane for most standers - individual foot bases can be adjusted for differential leg length- it was determined that load sensor form should be for each foot.

Physical therapists at Meeting street confirmed that left foot versus right foot and total weight borne would be the most useful measurements. Additionally, as most children are in orthotics that functionally lock their ankles, and the therapists thought that a front vs back loading measurement would not be exceptionally informative.

Since patients are strapped into the assisted standing device for security, and most standers do not have a protective lip in any case, there was no reason identified by PTs for a lip height requirement. However, height of this device was minimized based on feedback that thickness and size will reduce adoption.

To measure the amount of weight placed on each sensor, load cells are used. A load cell is a transducer. Specifically, it measures force and outputs it as an electrical signal. The most common load cells, and the one used in this design, utilizes strain gauges to measure applied forces. Force conversion is achieved by measuring the physical deformation of the internal strain gauge. When a strain gauge is bonded to a surface under stress, it deforms in unison with the surface, causing a change in electrical resistance. This change is proportional to the surface strain applied. Consequently, the change in resistance can be used to measure the deforming force. The deformation in either compression or tension causes a change in cross sectional area of the wiring of the strain gauge described by the relation:

$$R = \frac{\rho L}{A}$$

where R is the resistance of the circuit,ρ is the resistivity of the material (at a given temperature), L is the length of the wire and A is the cross-sectional area of the wire. This work is conducted at ambient temperature, and so the manipulation of the wiring's cross-sectional area, due to a deformation can be leveraged.

The deformation force will be from the weight on each load cell, and in this study, a participant standing on the sensor. To attain detail into the location of loading on a sensor, each sensor is with four load cells. Two load cells are installed towards the forefoot and two towards the hindfoot. Load cells

manufactured by Galoce (Appendix 2), were identified as having the appropriate rated capacity- 30kg - and with dimensions suited for these sensors.

Based on the constraints from the dimensions of the platform of the standers, as well as the dimensions of the load cells, the following dimensions (in millimeters) were determined for the footprint of the load sensors. This initial sketch (Figures 4 and 5) was proposed by Professor Joseph Crisco.

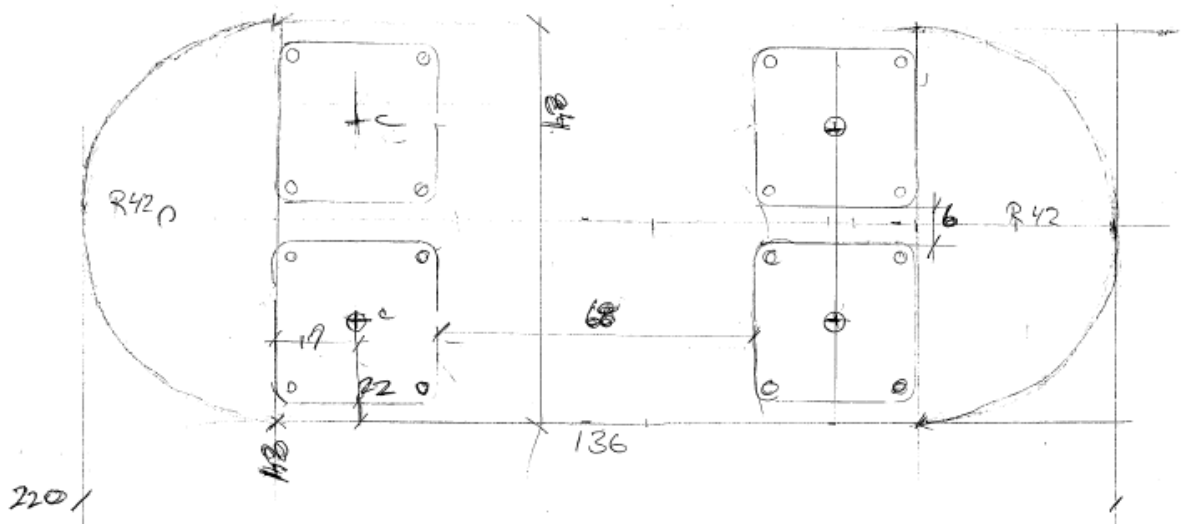

Figure 4: Dimensioned sketch of sensor - top view

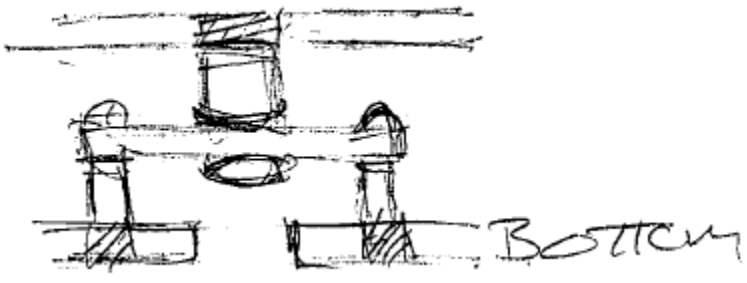

Figure 5: Original sketch of assembly of load cells and outer plate of sensor

Bill of Materials

The following materials list was used to construct each sensor. Materials were sourced from McMaster-Carr, unless otherwise noted.

Item	**Count**
18-8 Stainless Steel Hex Drive Flat Head Screw 10-32 thread size, 7/8" Long	4
18-8 Stainless-Steel Open-End Cap Nut 10-32 thread size	8
18-8 Stainless Steel Female Threaded Hex Standoff 3/16" Hex, 7/16" Long, 4-40 Thread	4
18-8 Stainless Steel Button Head Hex Drive Screw 4-40 Thread Size, 9/16" Long	4
18-8 Stainless Steel Female Threaded Hex Standoff 3/16" Hex, 1/4" Long, 2-56 Thread	16
18-8 Stainless Steel Button Head Hex Drive Screw 2-56 Thread Size, 7/16" Long	16
Multipurpose 6061 Aluminum, 1/8" Thick 220mmx84mm*	2
Galoce Micro load cell GM670 - 2.5mm**	4
NinjaFlex filament	1

Figure 6: Bill of Materials for Sensor

Electronics design and fabrication was managed by Bay Computer Associates. The external gaskets are 3D printed from NinjaFlex filament, a proprietary thermoplastic polyurethane (TPU), from NinjaTek. NinjaFlex ws chosen based on its flexibility, elasticity and high strength properties. It has been recommended for products that require flexibility and durability.

*Aluminum sheets were cut from a single 4" Wide, 1 Foot Long sheet milled using a Bridgeport miller in the Brown Design Workshop in the week of January 20th, 2020.

**Load cells manufactured by Galoce.

Additional items towards fabrication:

1. Ratchet Wrench, 1/4" Square Drive, 5" Overall Length
2. 6-Point Standard Socket, 1/4" Square Drive, 7/16" Size
3. Hex L-Key with Standard Tip, 1/16" Size, 3-1/16" Overall Length
4. Hex L-Key with Standard Tip, 1/8" Size, 3-15/16" Overall Length
5. Hex L-Key, Tip size 3/64”

Modeling and Assembly

Sensors were digitally modeled (Figure 7) using SolidWorks in November 2019 and assembled in March 2020 following completion of electronic components. Figures 8A, B and C provide orthographic views of this assembly.

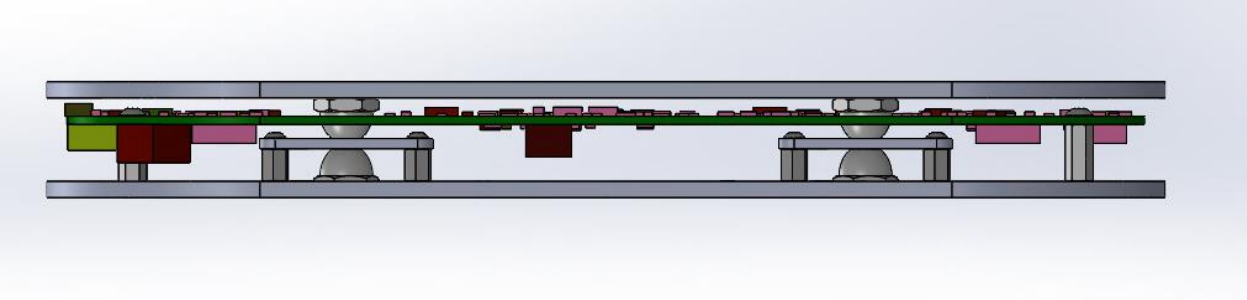

Figure 7: CAD assembly of sensor - right view

Figure 8A: Top view of Sensor

Figure 8B: Front view of Sensor

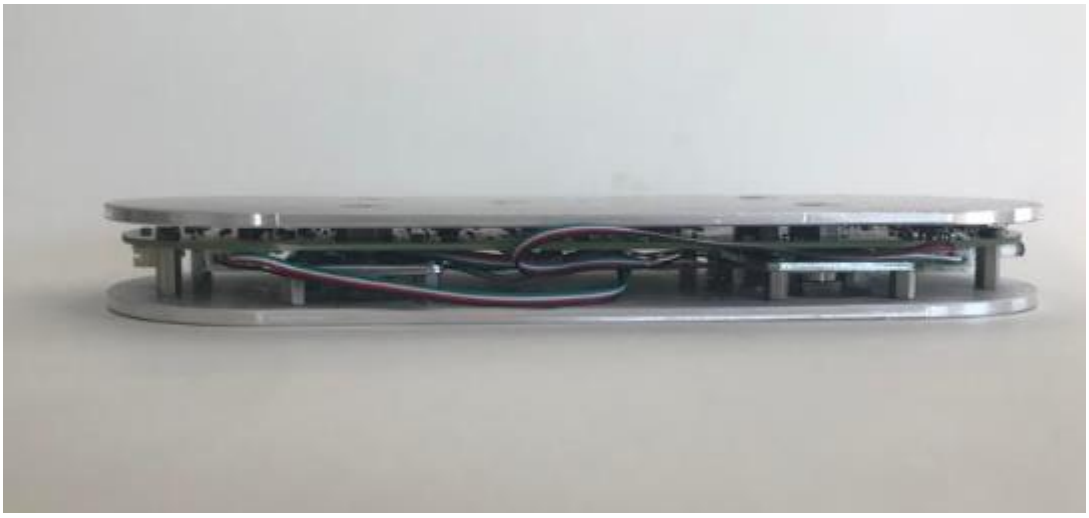

Figure 8C: Right view of Sensor, without gasket

Calibration

Data Collection

The following procedure was followed towards sensor calibration with dumbbell deadweights available at the Bioengineering Lab in Coro West, 1 Hoppin St, Providence, RI. All deadweight data collection was completed during the week of March 16th, 2020.

1. Sensor 1 was connected according to Data Collection-PuTTY guidelines described in Appendix 3.
2. Voltage readings from the sensor were collected for 30 seconds of time(t):
    a. t=0 to t=10, no weight on sensor
    b. t=11 to t=15, weight placed at the center of the sensor, upright, and balanced as needed.
    c. t=16 to t=25, weight was left to stand on the sensor.
    d. t=26 to t=30, weight was removed from the sensor.
3. PuTTY Data collection session was closed at the end of each trial.
4. Steps 2 and 3 were repeated 5 times each for the following 5 dumbbells:
    a. 0lbs
    b. 5lbs
    c. 10lbs
    d. 20lbs
    e. 35lbs
    f. 40lbs
5. Steps 1 through 4 were repeated for Sensor 2.

A sample of the output comma separated value (csv) file can be seen in Appendix 4.

Linear Response to Loading

MATLAB R2019b was used to process all the csv files collectively. Two MATLAB scripts were written. The first explores the following:

1. The linear model (in a least-squares sense) that relates the increase in resistance - and therefore voltage - of each load cell as well as the voltage increase from an applied load is recorded for the Sensors. These models are calculated for center loading as well as back loading system of loading. The correlation coefficient for each of the linear models is also calculated. The dumbbell deadweights were labelled in pounds and for the purpose of this study, a conversion factor of 4.448 Newtons/lb. was used.

Determination of this model supports the confirmation that the load and associated voltage increases across each of the 4 load cells, and the sum of the voltage increase (DelV), follows a linear relation that is consistent regardless of location of loading. Further, these linear equations are necessary to test the five assumptions of linearity for each sensor.

2. The 5 assumptions of linearity, and confirming they are valid for this model. The 5 assumptions of linearity are:
    a. Linear scatterplot of applied weight (independent variable) and increase in voltage from baseline (dependent variable). Additionally, this investigation further explores the differences in response between placing the deadweight at the center, and towards the back of each sensor. The repeatability of readings, independent of the location that a load makes contact on the sensor is necessary for implementation of this device. Figures 9A and 9B support this assumption for Sensor 1 and Sensor 2

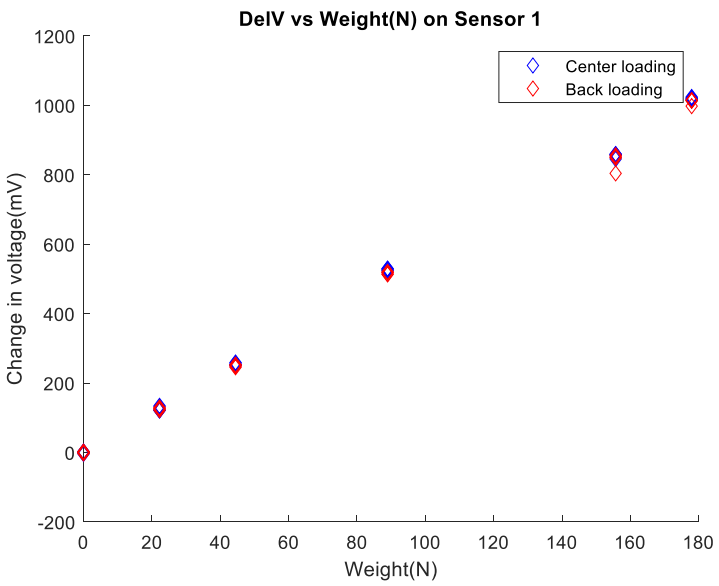

Figure 9A: - Linearity of center loading and backloading response for Sensor 1

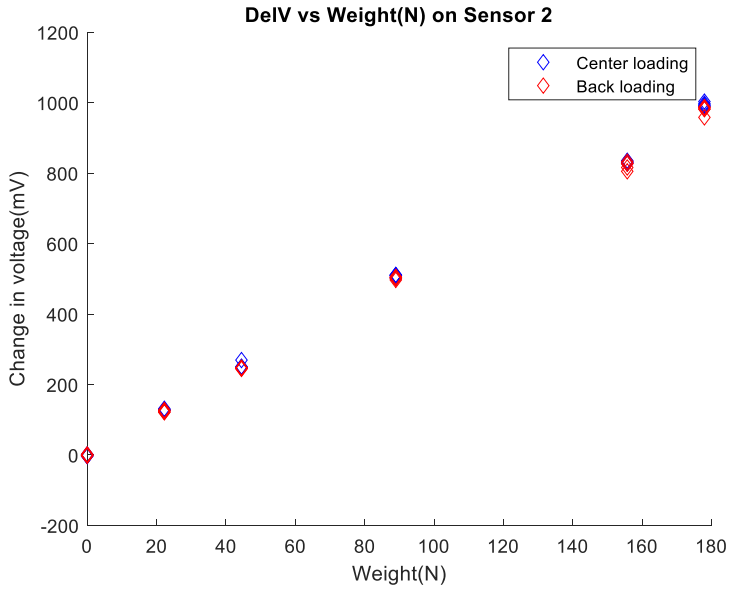

Figure 9B: Linearity of center loading and backloading response for the sensor 2

b. Mean of error = 0

c. Independence of error and independent variable

Sensor	Point of loading on sensor	E(Y-Y*)	Corr(Residuals,X)
1	Center	-1.1511e-13	-4.0921e-15
	Back	4.737e-14	3.6972e-15
2	Center	4.5475e-14	3.2208e-15
	Back	1.0895e-14	3.6972e-15

Figure 10: Table of expected value of residuals and correlation of residuals with applied weight

d. Homoscedasticity of errors. The error or "noise" of relationship between the applied weight and the response (voltage) is the same across all values of the applied weight

e. Normal distribution of errors.

The results of the investigations into the homoscedasticity of errors and normal distribution of errors can be found in Appendix 5.

3. Investigation into the reproducibility across sensors. The voltage increases of sensor 1 to center loading due to an applied load is compared to that of sensor 2. The same was done for backloading, and the following scatterplots (Figures 11A and 11B) illustrate the differences in sensor response. These figures suggest that the sensors produce near equivalent response to loading, particularly for lower amounts of force.

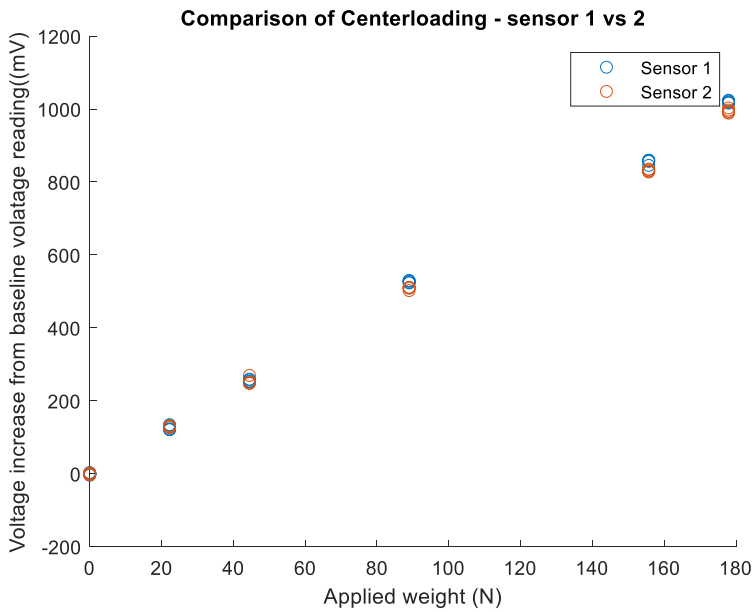

Figure 11A - Comparison of Sensor1 vs Sensor2 response to center loading

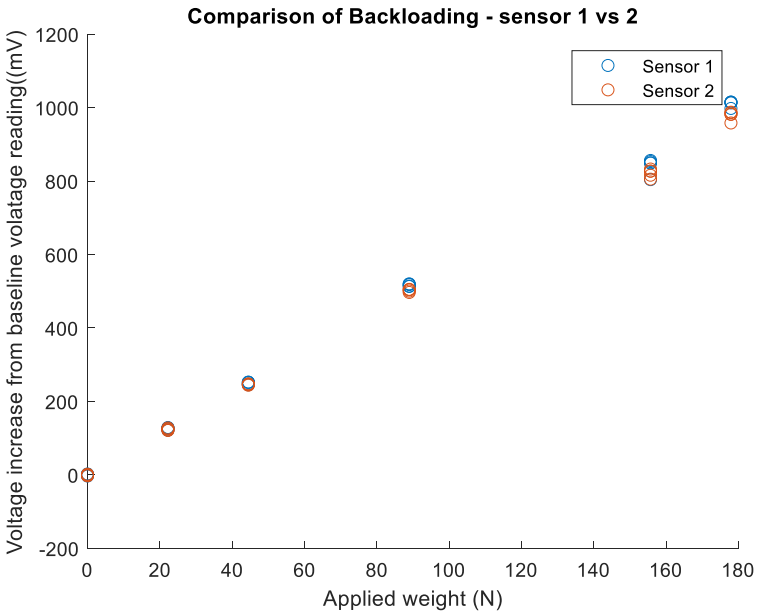

Figure 11B: - Comparison of Sensor1 vs Sensor2 response to back loading

The second analysis explores the effect of forcing the linear models generated through zero, which generates a new correlation coefficient, and a series of Bland Altman analyses. Appendix 6 displays the code for this process.

Forcing Models through Zero

This section of the data analysis begins with a recalibration of the linear model relating applied weight (independent variable) and voltage change (dependent variable), this time defining a point of the calibration curve as [0,0], that is applied weight =0N and sensor voltage increase = 0mV. A conversion factor of 4.448 Newtons/lb. was used. The calibration curve then takes the form y(mV)=m *x(N).

Sensor	**Point of loading on sensor**	**Slope (mV/N.)**
1	Center	5.669
	Back	5.597
2	Center	5.519
	Back	5.440

Figure 12: Table of calibration coefficients for Sensor 1 and Sensor 2

Again, the calibration equations are established under the assumptions described previously regarding linearity holds true.

Bland Altman Analysis of Agreement

Bland Altman (B-A) Analyses investigate the agreement between two quantitative methods of measurement. Frequently, studying the regression and correlation of the response of two methods are used for this purpose, but this investigation requires a comparability between two methods of measurement.

The B-A method explores agreement between two quantitative measurements by studying the mean difference. The result is a scatterplot, in which the Y axis shows the difference between the two paired measurements (A-B) and the X axis represents the average of these measures ((A+B)/2). That is to say, the difference of the two paired measurements is plotted against the mean of the two measurements. The Bland–Altman method calculates the mean difference between two methods of measurement (the 'bias'), and 95% limits of agreement as the mean difference (+/-2 standard deviations). It is expected that the 95% limits include 95% of differences between the two measurement methods (24).

I. Bland Altman Analysis - calibrated weights and Applied Deadweights

Using the linear models that take the form y=mx described in Section 4 of data analysis above, forcing through Zero, a Bland - Alman analysis was conducted between the applied deadweights and calibrated weights. For each sensor, to determine the “calibrated weight”, the calibration curve determined through using the center loading points (taking the form voltage = m*applied weight), was applied to voltage readings of the backloading system.

This is considered the result of a sensor’s method of measurement (in Newtons) that can be compared to the deadweight applied. This process is also completed for Sensor 2. The figures below describe the agreement of each sensor’s calibrated weight with the applied weight. As described previously for the purposes of this analysis a conversion factor of 4.448 Newtons/lb. was used.

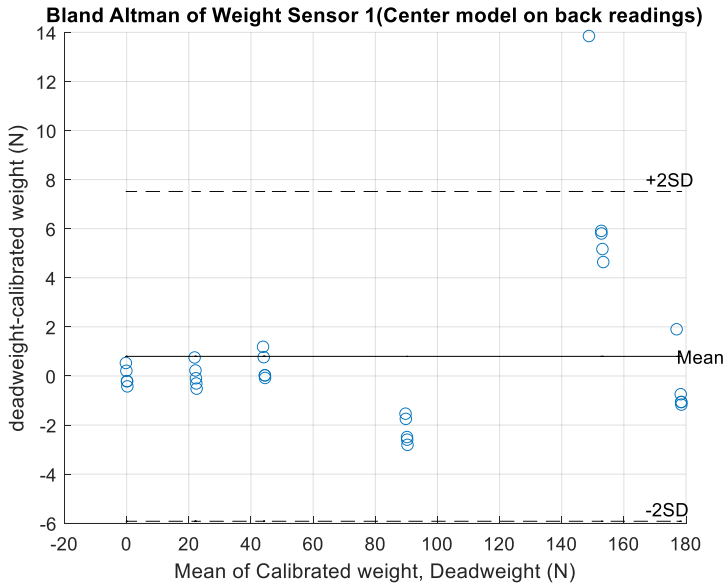

Figure 13A: B-A for Sensor 1 - Applying center loading calibration to backloading. Mean (+2SD, -2SD): 0.79902 (-5.9194, 7.5175)

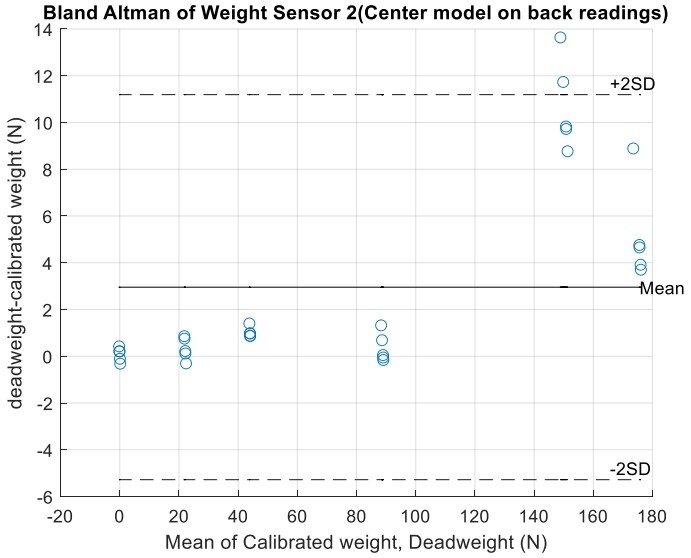

Figure 13B: B-A for Sensor 2 - Applying center loading calibration to backloading. Mean (+2SD, -2SD): 2.9548 (-5.2808,11.1904)

As can be seen from the figures above, for both Sensor 1 and Sensor 2, there is strong agreement between the calibrated and applied weights. Excluding 35lbs dumbbell loading, differences between the methods report less than a 10 N discrepancy. This holds true for the largest test weights.

II. Bland Altman Analysis - Center loading and Backloading Voltage increase

Paramount to the design verification is also assessing the agreement of the response (total voltage change) to backloading and center loading for each sensor. Since each deadweight was applied 5 times as backloading and 5 times as center loading, this was approached two ways.

A. For each sensor, the average voltage increases for each center loaded applied deadweight was calculated and compared to the same for backloading.

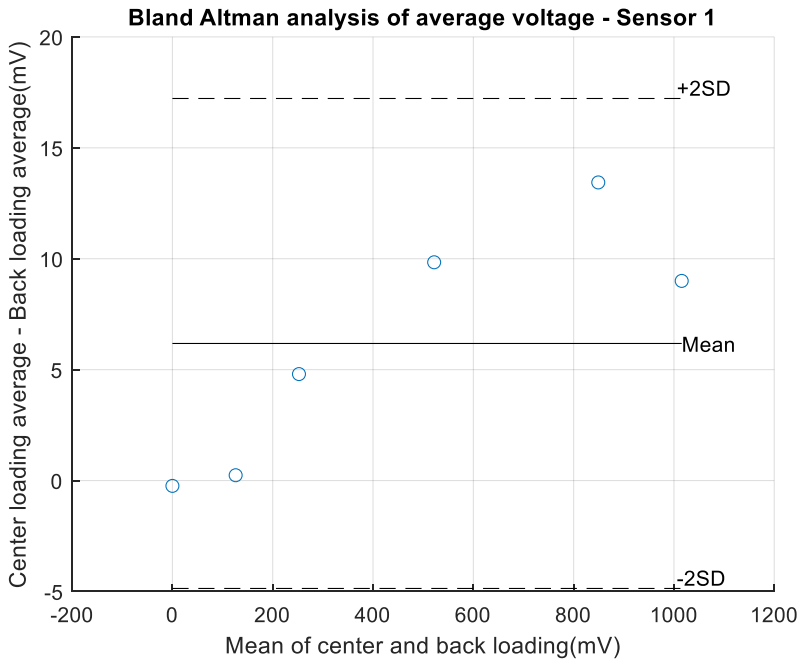

Figure 14A: BA of averages: center loading and backloading for Sensor 1. Mean (+2SD, -2SD): 6.18 (-4.8639, 17.2239)

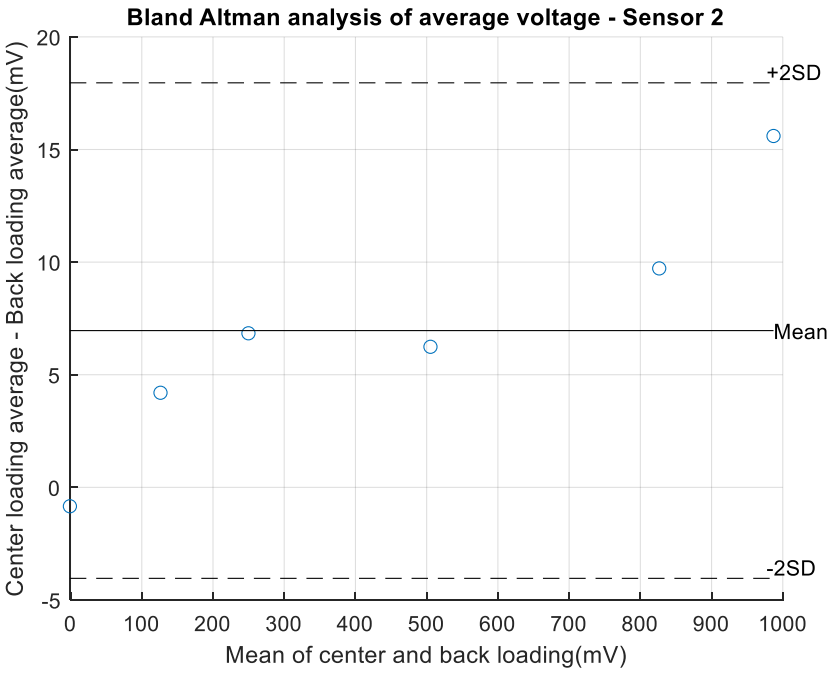

Figure 14B: BA of averages: center loading and backloading for Sensor 2. Mean (+2SD, -2SD): 6.96 (-4.0403, 17.9603)

B. Due to the independence of each of the 5 trials, the voltage increases from each trial under the center loading system was analyzed against each of the 5 trials with the same applied weight under the backloading system. Figures 13 and 14 highlight the comparisons for Sensor 1 and Sensor 2 respectively.

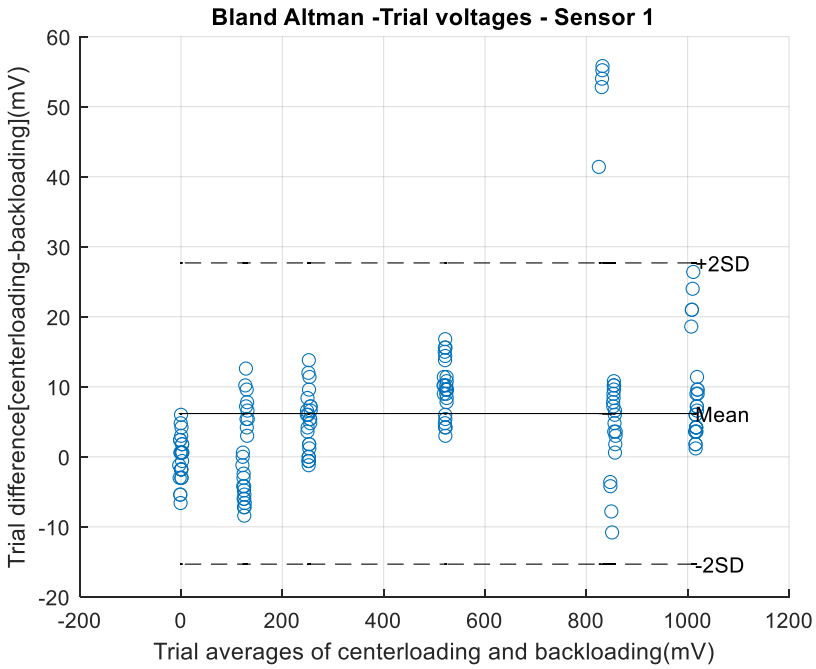

Figure 15A: BA of trials: center loading and backloading for Sensor 1. Mean (+2SD, -2SD): 6.18 (-15.3257, 27.6857)

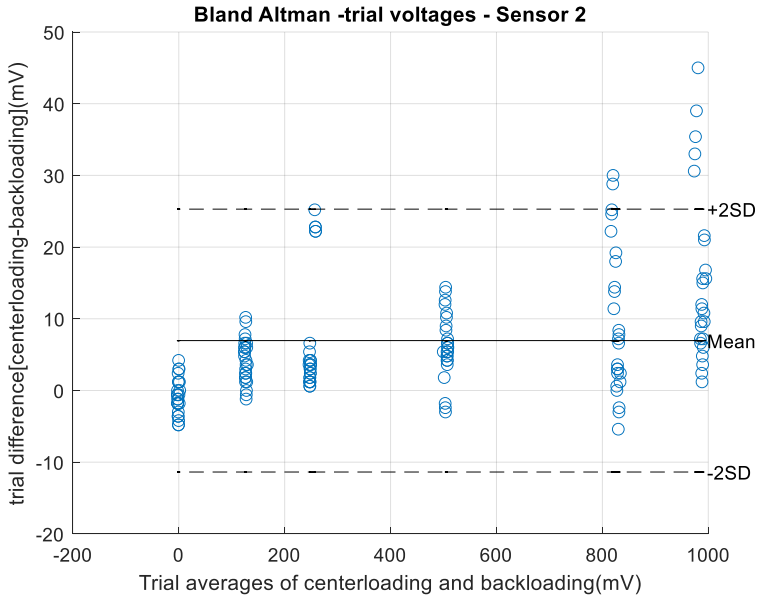

Figure 15B: BA of center loading and backloading for Sensor 2. Mean (+2SD, -2SD): 6.96 (-11.3728, 25.2928)

Whether the load was applied to the back or the center of the sensor, there was significantly larger variation among higher voltage readings than smaller voltage readings. This can be greatly attributed to deadweight dumbbells used to calibrate the sensors. In particular, the dumbbells have increasing "footprint" as the weight increases. The result of this was three-fold

1. Larger dumbbells, though placed at the back of the sensor, makes contact with a greater amount of the surface of the sensor.
2. Taller dumbbells have a surface is larger than sensor and are potentially less balanced, resulting in instability of voltage readings.
3. Heavier dumbbells result in greater experimental error in repetition in the exact position of the dumbbell's placement.

Feasibility Study

A feasibility study was granted full approval by the Rhode Island Hospital Institutional Review Board on February 11th, 2020. This study recruits fifteen participants, children between the ages of 8 and 18, currently attending Meeting Street, an independent school in Providence that enrolls children with moderate to severe developmental disabilities as well as children without disability.

This study was reviewed as a low risk pediatric study and the load sensor plate was granted an NSR (non-significant risk) determination based on the Instructions for Use documentation developed (Appendix 7). As a pediatric category A study, it is only necessary to get permission and a signature from one parent of each participant to enroll. Additionally, assent must be obtained from all capable participants.

All students being recruited for this study have cognitive disabilities of varying degrees. After signed parental consent is obtained, an IRB approved assent form will be read to the minor participant. If the participant can give consent using verbal or non-verbal methods, that will be documented. If the minor can use a stamp or other method to "sign" the assent form, that will be done. If the participant is not capable of one or both of these items, a Note to File will be generated stating that the

participant was unable to provide assent. After informed consent and assent (if possible) is obtained, up to five scheduled stander therapy sessions were attended to collect data for that participant.

The site of data collection is Meeting Street and was scheduled for in February and March 2020. However, this study will be postponed to the latter half of 2020. Participants will be placed in their prescribed stander, with the lead sensor already installed on the base platform of the assisted standing device. This study follows the standard of care for a stander therapy session.

In practice, this means that for each participant and session there was a prescribed duration and stander set up. However, this therapy process is also subject to patient tolerance. This assessment is done by the physical therapist present and is highly individualized.

Either on the day of the therapy session or later, the following data will be collected on each participant:

a) Initials
b) Age
c) Sex
d) Weight
e) Height
f) Difference in leg length, if present
g) Height of foam insert used, if present
h) Shoe size (subsequently approximated to foot length)

On the day of the stander session, the stander data collected will be:

a) Model
b) Manufacturer
c) Footplate dimensions
d) Relative height between footplates
e) Width between center of each footplate

Relevant participant information (described above) will be obtained from a database of student

information housed at Meeting Street and provided by Meeting Street staff.

Load associated with weight bearing on each foot will be continuously recorded throughout each stander therapy session. This recorded data will be tabulated and analyzed for trends associated with participant's and stander's collected information and recorded loads.

Additionally, approval to recruit a control group of children aged 8-17 years old of matched weight and height was also granted on March 27th, 2020. Participants in the control group are fully ambulatory students also enrolled at Meeting Street school. The control group is recruited to test the accuracy of the force plates by standing on the load sensor placed on the ground for the following positions:

1. weight centered on plate with both feet
2. front loaded with both feet (leaning weight forward to toes)
3. back loaded with both feet (weight leaning back towards heels)
4. outside load with both feet (weight leaning on the outer edge of both feet)
5. inside load with both feet (weight leaning on the inner edge of both feet)
6. center weighted right foot only
7. center weighted left foot only.

The preparation of documentation submitted to Rhode Island Hospital, including parental consent forms, participant assent forms and cover letter to parents were significantly supported by Cynthia Chrostek, Clinical Research Coordinator in the Department of Orthopedics.

Next Steps

Technical

To further validate the design of this weight sensor, the immediate next step is to recalibrate the sensor's response to loading, this time with precise loads as opposed to deadweights (dumbbells) using the Instron Universal Testing system. Again, the applied load on each sensor will be in the range of 0 to

100 kg, replicating the maximum loading from a person anticipated from the pediatric feasibility study approved.

Following this, conducting the approved feasibility study at Meeting Street will provide insight into the value and functioning of this sensor in clinical settings.

Commercial Potential

Commercialization potential is an area that is being explored. In January, this venture completed the regional New England Regional National Science Foundation's Innovation Corps (NE NSF I-Corps) Spark, a program that prepares scientists and engineers to extend their focus beyond the laboratory to accelerate the transfer of cutting-edge, NSF-funded research into commercial success. The Spark Program was an introduction to the customer discovery process, and this venture has been accepted to the NE NSF I-Corps Fusion program. The Fusion program provides a microgrant to support extensive customer discovery and is a stepping-stone to acceptance to the larger, national NSF I-Corps program, providing larger grant funding on the order of $50,000 and further expert support.

The New England Medical Innovation Center (NEMIC) hosts the Med Tech Leadership program, a comprehensive series of programs designed to train and educate Med Tech and digital health focused entrepreneurs and industry professionals. As a participant in this program, I have been exploring how to develop regulated products, examine current industry trends, and build the necessary skills to lead a fundable business.

This venture has also been accepted to two venture accelerators occurring over the next 4 months. The first, ongoing program is hosted by the Center for the Translation of Rehabilitation Engineering Advances and Technology (TREAT). TREAT is a collaborative consortium that provides education, expert consultation, and direct assistance to accelerate commercialization of rehabilitation and assistive technologies. TREAT is part of the National Institutes of Health (NIH) Medical Rehabilitation Research Resource Network (MR3). This venture has been accepted to TREAT’s Commercialization Advancement Cohort – an online, group-learning opportunity to define your path to market. Over the nine-week course

period beginning in April 2020, the Commercialization Advancement Cohort focuses on business development milestones and includes customer interviewing, medical device regulation and reimbursement, fundraising mechanisms, and developing financial pro forma.

Additionally, having been accepted to Breakthrough Lab (B-Lab), Brown University's 8-week summer accelerator program for Brown and RISD students developing high-impact ventures, this project is being positioned to explore the larger scale grants such as SBIR/STTR funding pathways. Through completing B-Lab I envision a rigorous approach to venture creation and see B-Lab as a springboard for ventures to go on to larger, national accelerator programs or directly to attract outside capital.

Finally, an application to the TREAT Rehabilitation Entrepreneur Fellowship Program has been submitted. The TREAT Entrepreneur Fellowship Program is an immersive cooperative educational and professional opportunity for individuals seeking experience in technology translation and commercialization. Fellows will join the TREAT leadership team and participate in regular meetings, including reviews, critiques, and assistance to the broad spectrum of rehabilitation and assistive technology commercialization projects that make up TREAT's clients. Additionally, Fellows also can advance their own technology.

References

1. Sackley C, Brittle N, Patel S, Ellins J, Scott M, Wright C, et al. The prevalence of joint contractures, pressure sores, painful shoulder, other pain, falls, and depression in the year after a severely disabling stroke. Stroke. 2008 Dec;39(12):3329–34.

2. Giangregorio L, McCartney N. Bone loss and muscle atrophy in spinal cord injury: epidemiology, fracture prediction, and rehabilitation strategies. J Spinal Cord Med. 2006;29(5):489–500.

3. The epidemiology of major joint contractures: a systematic review of the literature. - Abstract - Europe PMC [Internet]. [cited 2020 Apr 7]. Available from: https://europepmc.org/article/med/17179779

4. Paleg G, Livingstone R. Systematic review and clinical recommendations for dosage of supported home-based standing programs for adults with stroke, spinal cord injury and other neurological conditions. BMC Musculoskelet Disord. 2015 Nov 17;16:358.

5. CDC. Data and Statistics for Cerebral Palsy | CDC [Internet]. Centers for Disease Control and Prevention. 2020 [cited 2020 Apr 27]. Available from: https://www.cdc.gov/ncbddd/cp/data.html

6. Jan MMS. Cerebral Palsy: Comprehensive Review and Update. Ann Saudi Med. 2006;26(2):123–32.

7. Stroke Facts | cdc.gov [Internet]. 2020 [cited 2020 Apr 27]. Available from: https://www.cdc.gov/stroke/facts.htm

8. Hendricks HT, Limbeek J van, Geurts AC, Zwarts MJ. Motor recovery after stroke: A systematic review of the literature. Arch Phys Med Rehabil. 2002 Nov 1;83(11):1629–37.

9. Pediatric Standers | Special Needs Stander | Vitality Medical [Internet]. [cited 2020 Apr 27]. Available from: https://www.vitalitymedical.com/special-needs-pediatric-standers.html

10. Hoenig H, Murphy T, Galbraith J, Zolkewitz M. Case study to evaluate a standing table for managing constipation. SCI Nurs Publ Am Assoc Spinal Cord Inj Nurses. 2001;18(2):74–7.

11. Eng JJ, Levins SM, Townson AF, Mah-Jones D, Bremner J, Huston G. Use of prolonged standing for individuals with spinal cord injuries. Phys Ther. 2001 Aug;81(8):1392–9.

12. CONSIDERATIONS IN PASSIVE STANDING PROGRAMS FOR CLIENTS WHO ARE MEDICALLY FRAGILE. Pediatr Phys Ther. 2004 Spring;16(1):49.

13. Caulton JM, Ward KA, Alsop CW, Dunn G, Adams JE, Mughal MZ. A randomised controlled trial of standing programme on bone mineral density in non-ambulant children with cerebral palsy. Arch Dis Child. 2004 Feb;89(2):131–5.

14. Goemaere S, Van Laere M, De Neve P, Kaufman JM. Bone mineral status in paraplegic patients who do or do not perform standing. Osteoporos Int J Establ Result Coop Eur Found Osteoporos Natl Osteoporos Found USA. 1994 May;4(3):138–43.

15. Newman M, Barker K. The effect of supported standing in adults with upper motor neurone disorders: a systematic review. Clin Rehabil. 2012 Dec 1;26(12):1059–77.

16. Salem Y, Lovelace-Chandler V, Zabel RJ, McMillan AG. Effects of Prolonged Standing on Gait in Children with Spastic Cerebral Palsy. Phys Occup Ther Pediatr. 2010 Jan;30(1):54–65.

17. Robinson W, Smith R, Aung O, Ada L. No difference between wearing a night splint and standing on a tilt table in preventing ankle contracture early after stroke: a randomised trial. Aust J Physiother. 2008 Jan 1;54(1):33–8.

18. Glickman LB, Geigle PR, Paleg GS. A systematic review of supported standing programs. J Pediatr Rehabil Med. 2010;3(3):197–213.

19. Edwards LC, Layne CS. Effect of dynamic weight bearing on neuromuscular activation after spinal cord injury. Am J Phys Med Rehabil. 2007 Jun;86(6):499–506.

20. Herman D, May R, Vogel L, Johnson J, Henderson RC. Quantifying weight-bearing by children with cerebral palsy while in passive standers. Pediatr Phys Ther. 2007;19:283–7.

21. Kecskemethy HH, Herman D, May R, Paul K, Bachrach SJ, Henderson RC. Quantifying weight bearing while in passive standers and a comparison of standers. Dev Med Child Neurol. 2008;50(7):520–3.

22. Rifton | The Rifton TRAM (Transfer and Mobility device) goes beyond portable patient lifts [Internet]. [cited 2020 Apr 27]. Available from: https://www.rifton.com/products/lift-and-transfer-devices/rifton-tram

23. BiSym Scale | LiteGait.com [Internet]. [cited 2020 Apr 27]. Available from: https://litegait.com/products/bisym-scale

24. Giavarina D. Understanding Bland Altman analysis. Biochem Medica. 2015 Jun 5;25(2):141–51.

Appendix 1 – Stander Dimensions

Stander #	Prone/Supine	Footplate Length (in)	Footplate Width (heel) (in)	Footplate Width (forefoot) (in)	Lip Height (in)	Strap Invasion? (Y/N)	Footplate Shape
1	Supine	10.5	5	5	1	Y	Oval
2	Supine	9	4	4	0.8	Y	Oval
3	Prone	11.3	4.9	4.9	1.75	N	Oval
4	Prone	9	4.5	4.5	1.5	N	Oval
5	Supine	8.5	3	4.5	1.5	Y	Wedge
6	Prone	9.5	4	5	1.5	N	Wedge
7	Supine	8.25	3	4.5	1	N	Wedge
8	Supine	9.25	3.5	4.75	1.75	Y	Wedge
9	Supine	11.5	5	5	2.5	N	Oval
10	Supine	6.5	2.5	3.5	1.5	Y	Wedge
11	Prone	8.75	4	4	1.75	N	Oval
12	Supine	9	3.25	4.25	1.75	Y	Wedge

Figure A1-1: Table of stander dimensions

Appendix 2 – Galoce Micro Load Cell

GALOCE WEIGHING IS BELIEVING

Micro load cell

GML670

Installation size (mm):

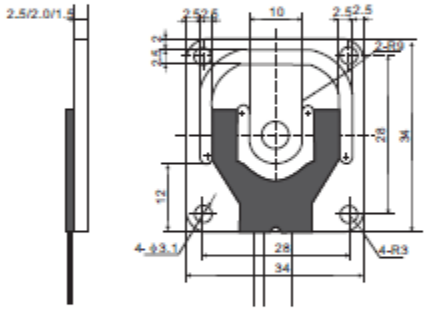

Features

- Material:alloy steel
- Application:hand scale,kitchen scale, microfore test equipment

Wiring Schematic Diag ram

Technical Specification

Rated capacity	10,30,50kg	Temp. effect on span	0.1%F.S/10℃
Rated output-FULL BRIDGE	1.5±0.2mV/V (50kg) 1.5±0.2mV/V (30kg) 1.0±0.2mV/V (10kg)	Temp. effect on zero	0.1%F.S/10℃
Rated output-HALF BRIDGE	0.8±0.15mV/V	Input resistance	1000±20Ω
Comprehensive error	0.05%F.S	Output resistance	1000±20Ω
Non-linearity	0.05%F.S	Insulation resistance	≥2000MΩ
Repeatability	0.05%F.S	Excitation voltage	3 ~ 10VDC
Hysteresis error	0.05%F.S	Compensated temp.range	-10 ~ +40℃
Creep	0.05%F.S/3min	Defend grade	IP66
Zero output	±0.3mV/V		

Xi 'an Gavin Electronic Technology Co., Ltd. T : +86 029-81292510 E: sales@galoce.com W: www.galoce.com

Figure A2-1: Technical documentation of Galoce Micro load cell

Appendix 3 – PuTTY Guide

In Device Manager:

When sensor is connected and on, under Ports, note the COM# (e.g. COM3)

In PuTTY Configuration (also be changed in terminal, by right clicking menu bar):

Under Session:

1. Serial line – set as COM# from Device Manager
2. Set speed to 115200
3. Set Connection type to Serial

Under Logging:

1. Set name to from .log to .csv and Browse to set location.csv

2 Name according to convention *weight_location_Trial_Sensor_mmddyy.csv* . For Trial 1 of a 5 lbs. weight placed at the center and collected on March 19, 2020 on sensor 1, it will be: *05lbs_CEN_T1_S103192020.csv*

Under Terminal

1. Check box for "Implicit CR in every LF"
2. Under Line discipline options >Local echo: **Force on**

Under Connection>Serial:

1. Confirm serial line, speed same as above
2. Data bits:8
3. Stop bits:1
4. Parity: None

5. Flow control: None

Alternatively, load a saved session, and set serial line and log file name

In Terminal

If new session:

1. Type "?", press Return
2. After lines of instructions appear type "mOn *frequency".*

    - A frequency of 1000=1 Hz

3. Press Return
4. Close terminal when done, data will be saved to location specified before

If not a new session, data collection begins automatically.

Appendix 4 – Sample Data Collection File

=~=~=~=~=~=~=~=~=~=~=~=~=~= PuTTY log 2020.03.20 13:33:23 =~=~=~=~=~=~=~=~=~=~=~=~=~=				
210mV 186mV 378mV 444mV 1218mV				
216mV 186mV 378mV 450mV 1230mV				
210mV 192mV 378mV 444mV 1224mV				
210mV 186mV 372mV 444mV 1212mV				
216mV 186mV 384mV 450mV 1236mV				
216mV 186mV 378mV 444mV 1224mV				
210mV 186mV 384mV 444mV 1224mV				
210mV 186mV 378mV 438mV 1212mV				
210mV 192mV 378mV 438mV 1218mV				
216mV 186mV 372mV 450mV 1224mV				
216mV 186mV 372mV 444mV 1218mV				
210mV 180mV 378mV 444mV 1212mV				
390mV 216mV 378mV 450mV 1434mV				
246mV 510mV 318mV 492mV 1566mV				
318mV 636mV 336mV 516mV 1806mV				
270mV 612mV 330mV 528mV 1740mV				
258mV 612mV 336mV 534mV 1740mV				
270mV 594mV 342mV 534mV 1740mV				
264mV 600mV 342mV 528mV 1734mV				
258mV 600mV 342mV 534mV 1734mV				
264mV 606mV 348mV 534mV 1752mV				
264mV 600mV 336mV 534mV 1734mV				
264mV 606mV 342mV 540mV 1752mV				
264mV 606mV 348mV 534mV 1752mV				
264mV 606mV 342mV 534mV 1746mV				
264mV 600mV 336mV 528mV 1728mV				
264mV 600mV 342mV 534mV 1740mV				
264mV 600mV 336mV 528mV 1728mV				
264mV 606mV 342mV 534mV 1746mV				

Figure A4-1: Sample table of voltage response from Sensor loading tests

Appendix 5 – Homoscedasticity and Normality Assumptions of Linearity

Results of the exploration into the homoscedasticity and normality assumptions of linearity of the relationship between applied weight and response of voltage increase.

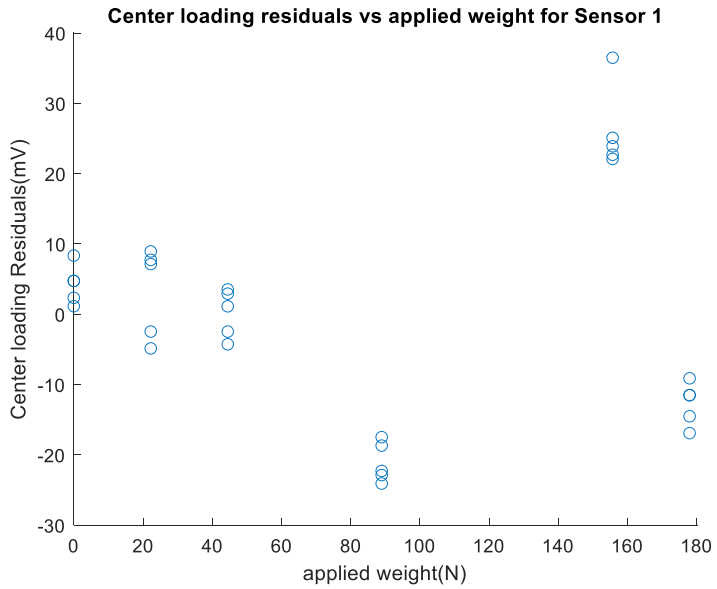

Figure A5-1 Scatterplot of applied deadweight and residuals of center loading Sensor 1

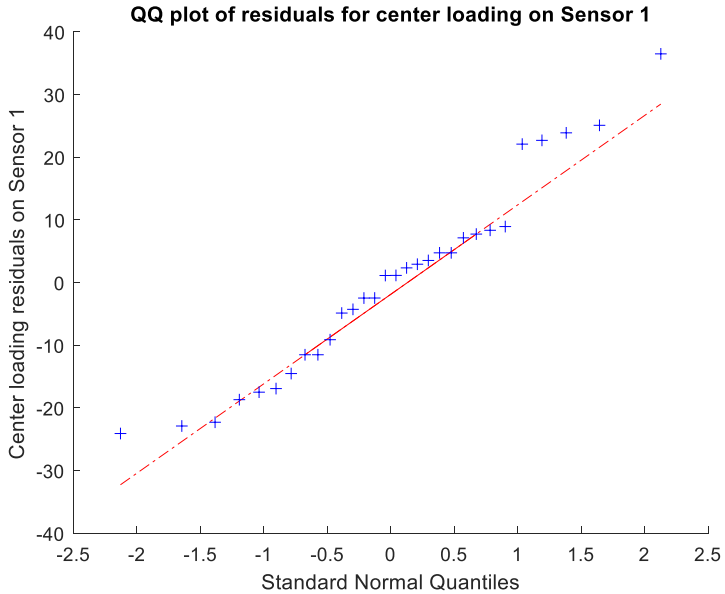

Figure A5-2 Quantile-Quantile plot: Normality of errors for center loading Sensor 1

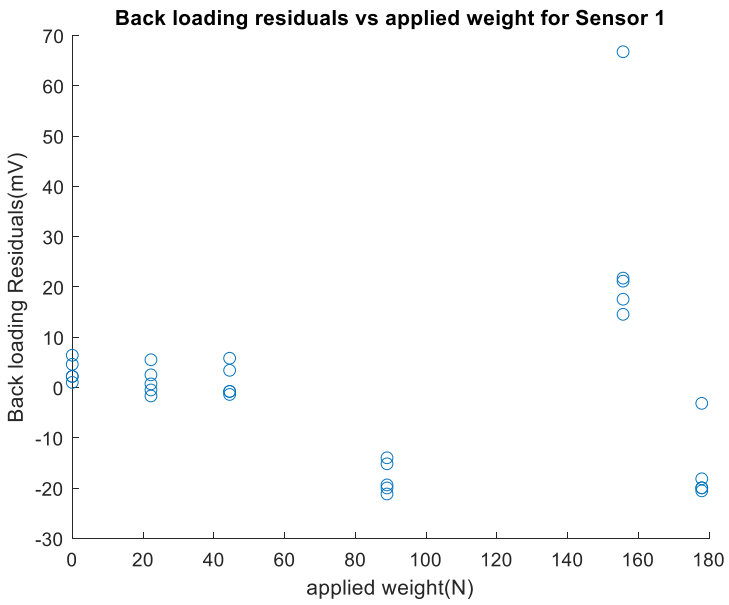

Figure A5-3 Scatterplot of applied deadweight and residuals of back loading Sensor 1

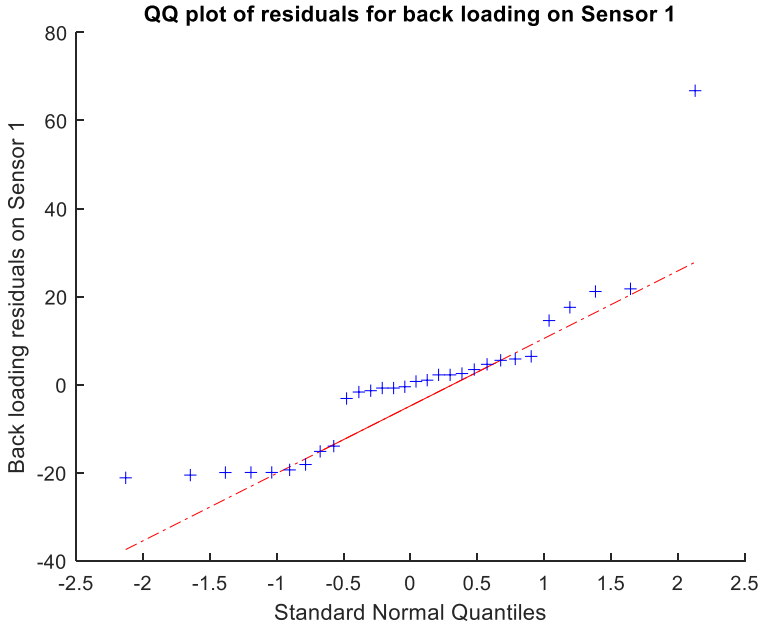

Figure A5-4 Quantile-Quantile plot: Normality of errors for backloading Sensor 1

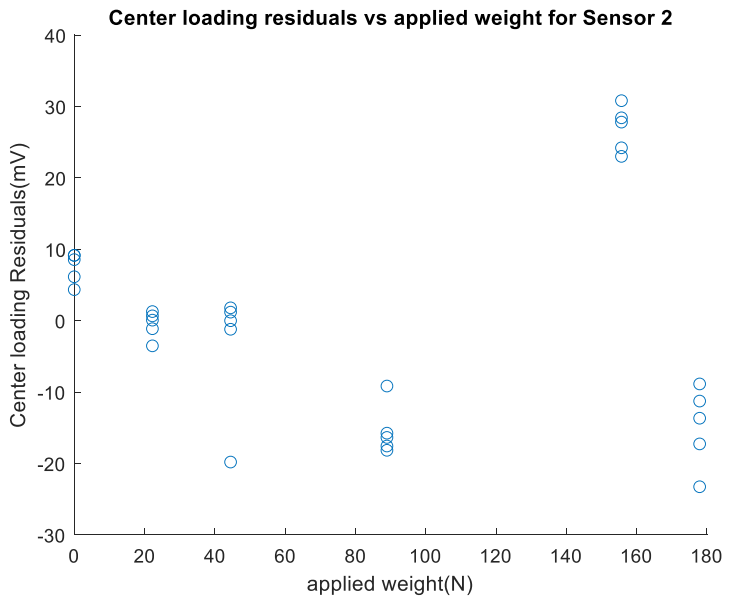

Figure A5-5 Scatterplot of applied deadweight and residuals of center loading Sensor 2

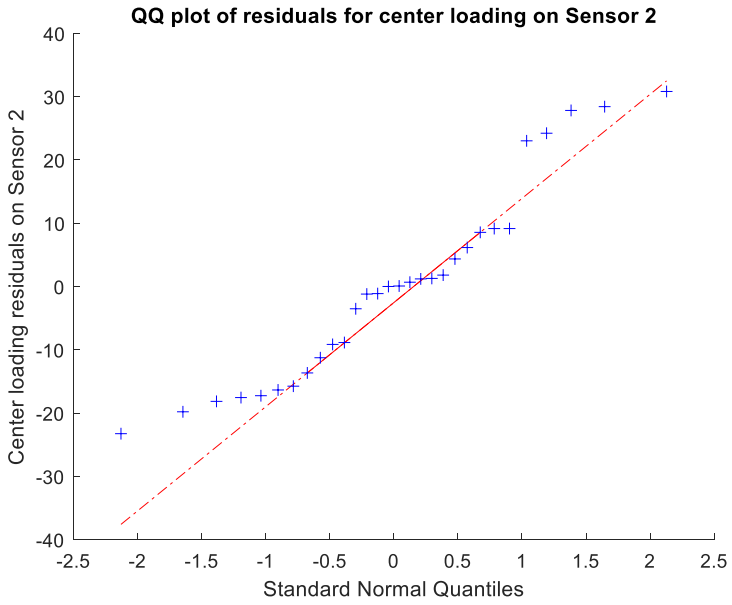

Figure A5-6 Quantile-Quantile plot: Normality of errors for center loading Sensor 2

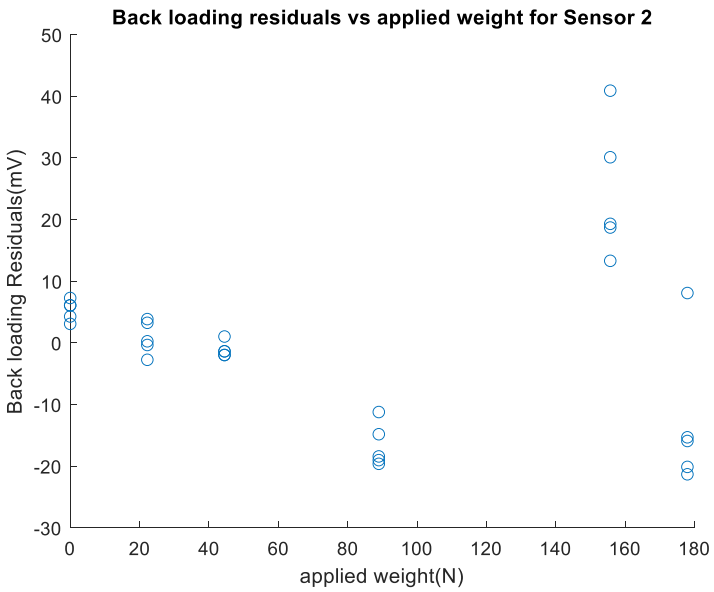

Figure A5-7 Scatterplot of applied deadweight and residuals of backloading Sensor 2

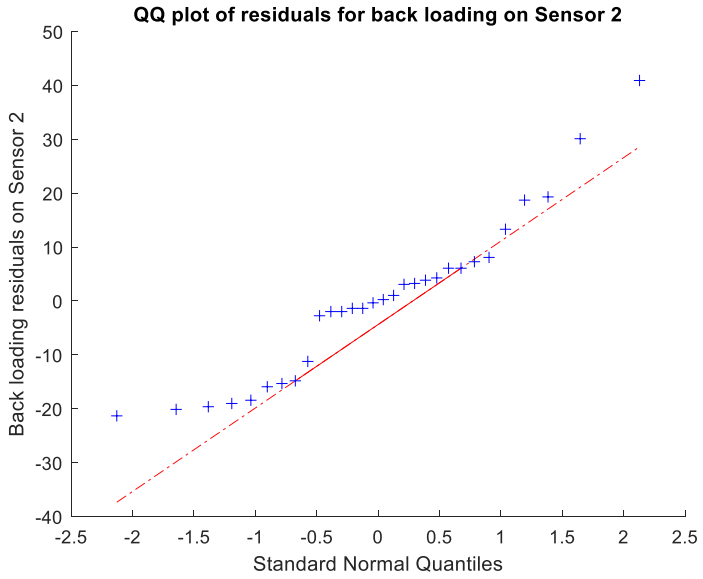

Figure A5-8 Quantile-Quantile plot: Normality of errors for backloading Sensor 2

Appendix 6 – MATLAB Code for Sensor Calibration and Bland-Altman

Below is the MATLAB code written to complete sensor calibration and Bland-Altman analyses.

```
% Specify the folder where the files live.
myFolder = 'C:\Users\jrdan\OneDrive\Documents\Grad school stuff\Weight
sensor\Thesis\raw data\Deadweight_tests\All_Sensors';
% Get list of all files in the folder with the desired file name pattern.
filePattern = fullfile(myFolder, '*.csv');
theFiles = dir(filePattern);

%making a table the length of all files, and 8 columns to hold all data
allDelV_weight_loc_senNum=zeros(length(theFiles),8);

% Make a matrix of doubles of all files
for k = 1 : length(theFiles)

  baseFileName = theFiles(k).name;
  fullFileName = fullfile(myFolder, baseFileName);
  fprintf(1, 'Now reading %s\n', fullFileName);

  %file processing
  dataRaw =readtable(baseFileName);
  dataRaw(1,:) = [];
  dataRaw(:,5)=[];
  dataRaw(end,:) = [];

  %remove mV units, change to doubles for calculations
  dataRaw = table2array(dataRaw);
  dataRaw = strrep(dataRaw,'mV','');
  dataRaw = cellfun(@str2double,dataRaw);

  %average first 10 readings of LC, set as baseline,normalize
  %10 seconds of collected data - first 5 columns of allDelV_w_loc
  baseV = mean(dataRaw(1:10,:));
  weightV = mean(dataRaw(16:25,:));
  DelV = weightV-baseV;

  %get weight from file name - will be column 6
  weight = str2double(fullFileName(end-25:end-24));

  %get location of weight from file name - will be column 7
  loading_location = fullFileName(end-19:end-17);

  %assign location integer for table
  if loading_location == 'CEN'
       location = 1; %column 7, the location column, assigned 1 if center
loaded
  else
       location = 2;% and 2 if back loaded (weight placed at the back)
  end
```

```
  %get sensor number from file name - will be column 8
  sensor = str2double(fullFileName(end-11));

  DelV_weight_loc_senNum = [DelV, weight, location, sensor];

  allDelV_weight_loc_senNum(k,:) = (DelV_weight_loc_senNum);

end
%Graphs x axis is Col 6 (applied weight).
added_weight = allDelV_weight_loc_senNum(:,6);

%Y axis is Col 1-5 (voltage change)
total_volt_change = allDelV_weight_loc_senNum(:,5);
LC1_volt_change = allDelV_weight_loc_senNum(:,1);
LC2_volt_change = allDelV_weight_loc_senNum(:,2);
LC3_volt_change = allDelV_weight_loc_senNum(:,3);
LC4_volt_change = allDelV_weight_loc_senNum(:,4);

%Criteria for linear modeling and scatterplots
%Criteria 1 is for Center loading(Col 7 = '1') on Sensor 1(Col 8 = '1')
crit1 = (allDelV_weight_loc_senNum(:,7)==1
&(allDelV_weight_loc_senNum(:,8)==1));
%Criteria 2 is for Back loading(Col 7 = '2') on Sensor 1(Col 8 = '1')
crit2 = (allDelV_weight_loc_senNum(:,7)==2
&(allDelV_weight_loc_senNum(:,8)==1));
%Criteria 3 is for Center loading(Col 7 = '1') on Sensor 2(Col 8 = '2')
crit3 = (allDelV_weight_loc_senNum(:,7)==1
&(allDelV_weight_loc_senNum(:,8)==2));
%Criteria 4 is for Back loading(Col 7 = '2') on Sensor 2(Col 8 = '2')
crit4 = (allDelV_weight_loc_senNum(:,7)==2
&(allDelV_weight_loc_senNum(:,8)==2));

conv = 4.448; %conversion factor for lbs to newtons (N/lb)

%Calculate linear model (in a least-squares sense) using fitlm function
%for each loading placement (back and front). Forcing through Zero
fprintf('\nThis is the linear models section - forcing through zero:\n')
for sensor=1:2 %2 sensors
    if sensor==1
       fprintf('These are linear models for Sensor 1:\n')
       %determining linear model coefficients and correlation
       center_model_S1=
fitlm(added_weight(crit1),total_volt_change(crit1),'y~x1-1');
       back_model_S2 =
fitlm(added_weight(crit2),total_volt_change(crit2),'y~x1-1');
       disp(['Equation for center loading is y(mV) = '
num2str(center_model_S1.Coefficients.Estimate) '*x(lbs)' ])
       disp(['Equation for center loading is y(mV) = '
num2str((center_model_S1.Coefficients.Estimate)/conv) '*x(N)' ])
       disp(['The correlation for center loading is '
num2str(center_model_S1.Rsquared.Adjusted)])
       disp(['Equation for back loading is y(mV) = '
num2str(back_model_S2.Coefficients.Estimate) '*x(lbs)' ])
       disp(['Equation for back loading is y(mV) = '
num2str((back_model_S2.Coefficients.Estimate)/conv) '*x(N)' ])
```

```
        disp(['The correlation for back loading is '
num2str(back_model_S2.Rsquared.Adjusted)])

    else
        fprintf('\nThese are linear models for Sensor 2:\n')
        % values for center loading sensor 2
        % values for back loading sensor 2
        %determining linear model coefficients and correlation
        center_model_S2=
fitlm(added_weight(crit3),total_volt_change(crit3),'y~x1-1');
        back_model_S2 =
fitlm(added_weight(crit4),total_volt_change(crit4),'y~x1-1');
        disp(['Equation for center loading is y(mV) = '
num2str(center_model_S2.Coefficients.Estimate) '*x(lbs)' ])
        disp(['Equation for center loading is y(mV) = '
num2str((center_model_S2.Coefficients.Estimate)/conv) '*x(N)' ])
        disp(['The correlation for center loading is '
num2str(center_model_S2.Rsquared.Adjusted)])
        disp(['Equation for back loading is y(mV) = '
num2str(back_model_S2.Coefficients.Estimate) '*x(lbs)' ])
        disp(['Equation for back loading is y(mV) = '
num2str((back_model_S2.Coefficients.Estimate)/conv) '*x(N)' ])
        disp(['The correlation for back loading is '
num2str(back_model_S2.Rsquared.Adjusted)])
    end

end
%}

%Bland Altman analysis of weights (deadweight vs calibrated weight)
fprintf('\nThis is the Bland Altman section for weights:\n')
for sensor=1:2

    if sensor==1
        deadweight = conv*(added_weight(crit1));
        fitted_weight =
conv*(total_volt_change(crit2)/center_model_S1.Coefficients.Estimate);
        diff = deadweight - fitted_weight;
        avg_dw_fitted = (deadweight+fitted_weight)/2;
        md = nanmean(diff);                % Mean of difference between
instruments
        sd = nanstd(diff);                 % Std dev of difference between
instruments
        scatter(avg_dw_fitted,diff,'o')    % Bland Altman plot
        hold on,plot(avg_dw_fitted,md*ones(1,length(avg_dw_fitted)),'-
k')     % Mean difference line
        text(avg_dw_fitted(end),md,'Mean')
        plot(avg_dw_fitted,((2*sd)+md)*ones(1,length(avg_dw_fitted)),'--
k')  %Mean plus 2*SD line
        text(avg_dw_fitted(end)-10,((2*sd)+md+0.5),'+2SD')
        plot(avg_dw_fitted,((-2*sd)+md)*ones(1,length(avg_dw_fitted)),'--
k')  % Mean minus 2*SD line
        text(avg_dw_fitted(end)-10,((-2*sd)+md+0.5),'-2SD')
        grid on
        xlabel('Mean of Calibrated weight, Deadweight (N)');
        ylabel('deadweight-calibrated weight (N)')
```

```
        title('Bland Altman of Weight Sensor 1(Center model on back
readings)')
        disp(['Sensor 1: Mean(+2SD, -2SD): ', num2str(md),'(',num2str((-
2*sd)+md),',',num2str((2*sd)+md),')']);
        figure

    else
        deadweight = conv*(added_weight(crit3));
        fitted_weight =
conv*(total_volt_change(crit4)/center_model_S1.Coefficients.Estimate);
        diff = deadweight - fitted_weight;
        avg_dw_fitted = (deadweight+fitted_weight)/2;
        md = nanmean(diff);                % Mean of difference between
instruments
        sd = nanstd(diff);                 % Std dev of difference between
instruments
        scatter(avg_dw_fitted,diff,'o')    % Bland Altman plot
        hold on,plot(avg_dw_fitted,md*ones(1,length(avg_dw_fitted)),'-
k')         % Mean difference line
        text(avg_dw_fitted(end),md,'Mean')
        plot(avg_dw_fitted,((2*sd)+md)*ones(1,length(avg_dw_fitted)),'--
k')       %Mean plus 2*SD line
        text(avg_dw_fitted(end)-10,((2*sd)+md+0.5),'+2SD')
        plot(avg_dw_fitted,((-2*sd)+md)*ones(1,length(avg_dw_fitted)),'--
k')       % Mean minus 2*SD line
        text(avg_dw_fitted(end)-10,((-2*sd)+md+0.5),'-2SD')
        grid on
        xlabel('Mean of Calibrated weight, Deadweight (N)');
        ylabel('deadweight-calibrated weight (N)')
        title('Bland Altman of Weight Sensor 2(Center model on back
readings)')
        disp(['Sensor 2: Mean(+2SD, -2SD): ', num2str(md),'(',num2str((-
2*sd)+md),',',num2str((2*sd)+md),')']);
        figure
    end


end
%}

%Bland Altman analysis of average voltage - centerloading vs backloading
fprintf('\nThis is the Bland Altman section for average voltages:\n')
for sensor=1:2
   center_avg_S1 = mean(reshape(total_volt_change(crit1),[5,6]));
   back_avg_S1= mean(reshape(total_volt_change(crit2),[5,6]));
   center_avg_S2=mean(reshape(total_volt_change(crit3),[5,6]));
   back_avg_S2=mean(reshape(total_volt_change(crit4),[5,6]));

    if sensor==1
        volt_avg_diff = center_avg_S1 - back_avg_S1;
        volt_avg = (center_avg_S1 + back_avg_S1)/2;
        md = nanmean(volt_avg_diff);               % Mean of difference
between instruments
        sd = nanstd(volt_avg_diff);                % Std dev of difference
between instruments
        scatter(volt_avg,volt_avg_diff,'o')    % Bland Altman plot
```

```
        hold on,plot(volt_avg,md*ones(1,length(volt_avg)),'-k')     % Mean
difference line
        text(volt_avg(end),md,'Mean')
        plot(volt_avg,((2*sd)+md)*ones(1,length(volt_avg)),'--k')  %Mean plus
2*SD line
        text(volt_avg(end)-10,((2*sd)+md+0.5),'+2SD')
        plot(volt_avg,((-2*sd)+md)*ones(1,length(volt_avg)),'--k')  % Mean
minus 2*SD line
        text(volt_avg(end)-10,((-2*sd)+md+0.5),'-2SD')
        grid on
        xlabel('Mean of center and back loading(mV)')
        ylabel('Center loading average - Back loading average(mV)')
        title('Bland Altman analysis of average voltage - Sensor 1')
        disp(['Sensor 1: Mean(+2SD, -2SD): ', num2str(md),'(',num2str((-
2*sd)+md),',',num2str((2*sd)+md),')']);
        figure

   else
        volt_avg_diff = center_avg_S2 - back_avg_S2;
        volt_avg = (center_avg_S2 + back_avg_S2)/2;
        md = nanmean(volt_avg_diff);                % Mean of difference
between instruments
        sd = nanstd(volt_avg_diff);                 % Std dev of difference
between instruments
        scatter(volt_avg,volt_avg_diff,'o')    % Bland Altman plot
        hold on,plot(volt_avg,md*ones(1,length(volt_avg)),'-k')     % Mean
difference line
        text(volt_avg(end),md,'Mean')
        plot(volt_avg,((2*sd)+md)*ones(1,length(volt_avg)),'--k')  %Mean plus
2*SD line
        text(volt_avg(end)-10,((2*sd)+md+0.5),'+2SD')
        plot(volt_avg,((-2*sd)+md)*ones(1,length(volt_avg)),'--k')  % Mean
minus 2*SD line
        text(volt_avg(end)-10,((-2*sd)+md+0.5),'-2SD')
        grid on
        xlabel('Mean of center and back loading(mV)')
        ylabel('Center loading average - Back loading average(mV)')
        title('Bland Altman analysis of average voltage - Sensor 2')
        disp(['Sensor 2: Mean(+2SD, -2SD): ', num2str(md),'(',num2str((-
2*sd)+md),',',num2str((2*sd)+md),')']);
        figure
   end

end
%}

%Bland Altman analysis of individual trial voltages - centerloading vs
backloading,
%no averaging
fprintf('\nThis is the Bland Altman section for individual trial
voltages:\n')
for sensor=1:2

    all_difference = zeros(25,6);
    all_mean = zeros(25,6);
    if sensor==1
```

```
    center_volt =reshape(total_volt_change(crit1),[5,6]);
    back_volt = reshape(total_volt_change(crit2),[5,6]);

        for trial=1:5
            row_difference=center_volt(trial,:)-back_volt;
            all_difference(((trial*5)-4):trial*5,:) = row_difference;
            row_mean = (center_volt(trial,:)+back_volt)/2;
            all_mean(((trial*5)-4):trial*5,:)=row_mean;
        end
     element_means = reshape(all_mean,[150,1]);
     element_diffs = reshape(all_difference,[150,1]);
     md = nanmean(element_diffs);                % Mean of difference between
instruments
     sd = nanstd(element_diffs);                 % Std dev of difference
between instruments
     scatter(element_means,element_diffs,'o')    % Bland Altman plot
     hold on,plot(element_means,md*ones(1,length(element_means)),'-
k')         % Mean difference line
     text(element_means(end)+5,md,'Mean')
     plot(element_means,((2*sd)+md)*ones(1,length(element_means)),'--
k')      %Mean plus 2*SD line
     text(element_means(end)+5,((2*sd)+md),'+2SD')
     plot(element_means,((-2*sd)+md)*ones(1,length(element_means)),'--
k')      % Mean minus 2*SD line
     text(element_means(end)+5,((-2*sd)+md),'-2SD')
     grid on
     ylabel('Trial difference[centerloading-backloading](mV)')
     xlabel('Trial averages of centerloading and backloading(mV)')
     title('Bland Altman -Trial voltages - Sensor 1')
     disp(['Sensor 1: Mean(+2SD, -2SD): ', num2str(md),'(',num2str((-
2*sd)+md),',',num2str((2*sd)+md),')']);
     figure

    else%sensor==2
    center_volt =reshape(total_volt_change(crit3),[5,6]);
    back_volt = reshape(total_volt_change(crit4),[5,6]);

        for trial=1:5
            row_difference=center_volt(trial,:)-back_volt;
            all_difference(((trial*5)-4):trial*5,:) = row_difference;
            row_mean = (center_volt(trial,:)+back_volt)/2;
            all_mean(((trial*5)-4):trial*5,:)=row_mean;
        end
     element_means = reshape(all_mean,[150,1]);
     element_diffs = reshape(all_difference,[150,1]);
     md = nanmean(element_diffs);                % Mean of difference between
instruments
     sd = nanstd(element_diffs);                 % Std dev of difference
between instruments
     scatter(element_means,element_diffs,'o')    % Bland Altman plot
     hold on,plot(element_means,md*ones(1,length(element_means)),'-
k')         % Mean difference line
     text(element_means(end)+5,md,'Mean')
     plot(element_means,((2*sd)+md)*ones(1,length(element_means)),'--
k')      %Mean plus 2*SD line
     text(element_means(end)+5,((2*sd)+md),'+2SD')
```

```
     plot(element_means,((-2*sd)+md)*ones(1,length(element_means)),'--
k')       % Mean minus 2*SD line
     text(element_means(end)+5,((-2*sd)+md),'-2SD')
     grid on
     ylabel('trial difference[centerloading-backloading](mV)')
     xlabel('Trial averages of centerloading and backloading(mV)')
     title('Bland Altman -trial voltages - Sensor 2')
     disp(['Sensor 2: Mean(+2SD, -2SD): ', num2str(md),'(',num2str((-
2*sd)+md),',',num2str((2*sd)+md),')']);
     figure

    end
 end
%}
```

Appendix 7 – Instructions for Use document

Load Bearing Force Plate - Instructions for Use

1. General Instructions

Load bearing sensors are intended to be used as a tool for the measurement and recording of load bearing of patients undergoing routine stander therapy. The sensors should only be used with approved devices and accessories. This sensor technology gives the attending physiotherapist, researchers and clinicians a means of monitoring the extent of load bearing within a stander therapy session and over multiple stander therapy sessions. Load bearing helps generally in bone density development and stimulating muscle growth; however, these implants are intended only to assist in measurement of load bearing, not the activity itself. The physiotherapist, researcher and user otherwise must be thoroughly knowledgeable not only in the mechanical and electrical operation of the device, but also must be aware of the functionality of complementing connected digital tools.

2. Device Description

Top and bottom surfaces made from aluminum. b) Internal printed circuit board (PCB) made from fiberglass epoxy resin and circuits from copper. c) Load cells made from alloy steel. d)Standoffs, cap nuts and screws are made from stainless steel. d) External gasket, if present made from NinjaFlex, a proprietary thermoplastic polyurethane (TPU). e) Battery pack is IEC 62133 approved. g) The surface of the sensor is chemically passive.

3. Indications

Load bearing sensors are intended to be used as a tool to measure and record the magnitude and time period of load bearing for persons undergoing stander therapy.

4. Precautions and Warnings

Correct orientation and fixation of the sensor to the stander's foot platform is important. The potential for success of load bearing measurement is increased by this proper attachment. b) These devices can break when subjected to the load outside of defined limits. The limit for each sensor is 140kg.

c) Do not use sensor while being charged. d) Do not remove external gasket e) Do not get wet. If exposed to significant moisture, dry pat dry. f) Do not expose to direct sunlight for extended periods. g) . There is reverse/over voltage protection on the circuit's battery input. f) The main system power supply includes short circuit and internal thermal protection. The battery charger also has internal reverse current, short-circuit, and thermal protection.

5. Notes

The user should record and keep all information provided to the patient. It should be checked during use whether the patient tolerates the addition of the force plate to the stander platform and if force plate is in the appropriate orientation.

6. Possible Adverse Effects

No adverse effects are anticipated with proper use. Foot plate should be kept away from sources of excessive moisture, particularly when connected to electrical sources. Structural fidelity is not in place for excessive jumping, but only standing.

7. Cleaning and Sterilization

If external surface is exposed to biological sources, wipe down exterior with cloth dampened with disinfectant and scrub as necessary. If internal surfaces are exposed, complete cleaning of exterior and report incident to researcher. Place in area of isolation and follow protocol for disposal if exposed to hazardous materials.

8. Sensor Usage

Prior to patient beginning therapy session, arrange sensor on stander foot platform, ensuring proper orientation. Turn on the sensor and connect it to available computer with USB. Ensure sensor remains firmly fastened to stander foot platform after patient is placed in stander. Begin collecting load bearing data points and continue throughout the duration of therapy session. Immediately following therapy session, and patient leaving stander, remove USB connection to computer from sensor and detach sensor from foot platform. Turn off sensor when not in use.

9. Limited Warranty / Liability There is no warranty or liability as these are prototype devices with minimal risk.

10. Contact Information

    For additional information on this device, please contact:

    J.J. Trey Crisco, PhD

    office: 1 Hoppin Street, Suite 402C Coro West, Providence, RI 02903

    email: joseph_crisco@brown.edu

    web page: http://www.brownbiomechanics.org

    tel: 401-444-4231

    fax: 401-444-4418